26th INTERNATIONAL CONGRESS ON SOUND AND VIBRATION
7-11 July 2019, Montreal

RESPONSE VARIABILITY OF BROADBAND MULTI-FREQUENCY METASTRUCTURE FROM ADDITIVE MANUFACTURING

Adriano T. Fabro
Department of Mechanical Engineering, University of Brasilia, 70910-900, Brazil
adrianotf@gmail.com

Han Meng and Dimitrios Chronopoulos
Institute for Aerospace Technology & The Composites Group, University of Nottingham, NG8 1BB, UK
email: han.Meng@nottingham.ac.uk，dimitrios.chronopoulos @ nottingham.ac.uk

Additive manufacturing has been used to propose several designs of phononic crystals and metamaterials due to the low cost to produce complex geometrical features. However, like any other manufacturing process, it can introduce material and geometrical variability in the nominal design and therefore affect the structural dynamic performance. Locally resonant metamaterials are typically designed such that the distributed resonators have the same natural frequency or, in the case of rainbow metastructures, a well-defined spatial profile. In this work, manufacturing tolerances of beam samples produced from a Selective Laser Sintering process are assessed and variability levels are used to investigate the vibration suppression performance of broadband multi-frequency metastructures. Evenly spaced non-symmetric resonators are attached to a beam with U-shaped cross-section. An analytical model based on a transfer matrix approach is used to calculate transfer receptance due to a point time harmonic force. Moreover, a random field model is assumed based in previous experimental results and the effects of the correlation length, a measure of the spatial fluctuation, are also investigated for individual beams and also in terms of ensemble statistics. The obtained results are expected to be useful for further robust design in mass produced industrial applications.
Keywords: vibration attenuation, rainbow metamaterial, additive manufacturing, uncertainties

1. Introduction

Additive manufacturing (AM) has been used to propose several designs of phononic crystals and metamaterials due to the low cost to produce complex geometrical features and has the potential to make them feasible in several industrial applications [1] along with the use of smart structures (e.g. [2]). However, like any other manufacturing process, AM can introduce material and geometrical variability in the nominal design and therefore affect the structural dynamic performance. There is very little experimental work available in the literature investigating metamaterial performance for vibration attenuation applications (e.g. [3, 4]) and most of them do not consider the effects of spatially correlated disorder on the band gap. Overall, there is a need to investigate the effects of the manufacturing variability, which can causes a mistuning of the resonators or affects the coupling of the metastructures to the vibration source and receiver [5], on performance of metastructures.

In this work, manufacturing tolerances of beam samples produced from a Selective Laser Sintering process are assessed and variability levels are used to investigate the vibration suppression performance of broadband multi-frequency metastructures. Evenly spaced non-symmetric resonators are attached to a beam with U-shaped cross-section. An analytical model based on a transfer matrix approach is used to calculate transfer receptance due to a point time harmonic force. Moreover, a random field model is assumed based in previous experimental results [4] and the effects of the correlation length, a measure of the spatial fluctuation, are also investigated for individual beams and also in terms of ensemble statistics. The obtained results are expected to be useful for further robust design in mass produced industrial applications.

2. Metamaterial beam with non-symmetric resonators

In this section, the proposed metastructure and an analytical model for beam with two non-symmetric resonators is, shown in Figure 1, is briefly presented. The metastructure is composed of a total of 17 unit cells, with two non-symmetric cantilever-mass attached acting like local resonators, as presented in Figure 2. In the proposed design, each resonator can act independently such that it is possible to create two separate band gap regions, thus broadening the total attenuation band.

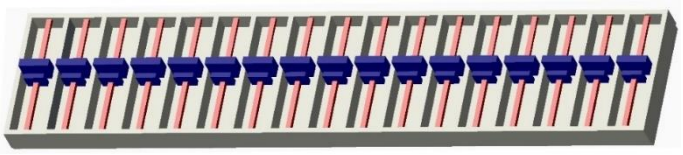

Figure 1: Schematic representations of the metamaterial beam with non-symmetric resonators at each unit cell.

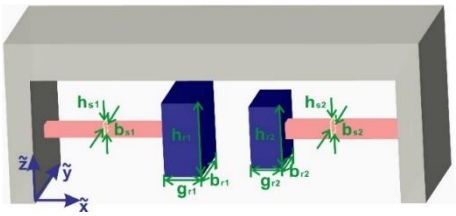

Figure 2: Schematic representations of the metamaterial unit cell with non-symmetric resonators.

An analytical model is proposed based on transfer matrix approach. It is assumed a Euler-Bernoulli beam theory for both the baseline structure and the cantilever-mass resonator. Each resonator is modelled as a beam attached to the baseline structure at one end and a lumped mass with negligible inertia at the other. The transversal displacement of the n^{th} unity cell is given by

$$w_{n,l} = \alpha_{n,l} e^{-ik\left(x-x_{n-1}\right)} + \beta_{n,l} e^{-k\left(x-x_{n-1}\right)} + \chi_{n,l} e^{ik\left(x-x_{n-1}\right)} + \varepsilon_{n,l} e^{k\left(x-x_{n-1}\right)}, \tag{1}$$

where …. . Continuity and equilibrium conditions are applied to find the transfer matrix from the first cell, at the left end to the n_{th} cell, such that

$$\begin{bmatrix} \alpha_{n+1,l} \\ \beta_{n+1,l} \\ \chi_{n+1,l} \\ \varepsilon_{n+1,l} \end{bmatrix} = \mathbf{T}_n \begin{bmatrix} \alpha_{n,l} \\ \beta_{n,l} \\ \chi_{n,l} \\ \varepsilon_{n,l} \end{bmatrix} = \mathbf{T}_n \mathbf{T}_{n\text{-}1} \cdots \mathbf{T}_1 \begin{bmatrix} \alpha_{1,l} \\ \beta_{1,l} \\ \chi_{1,l} \\ \varepsilon_{1,l} \end{bmatrix} \tag{2}$$

This formulation can be used to find the transfer receptance, i.e. the displacement at one end per unity force applied at the other end of the structure.

3. Manufacturing variability on the periodic design

In this section the material and geometrical variability introduced by the additive manufacturing process in the nominal design in discussed. It has been shown that the break of periodicity introduced by the spatial variability of material and geometrical properties of the metastructure creates a resonator mistuning which can induce wave trapping and thus greatly affecting the vibration attenuation performance by either band annihilation attenuation bandwidth widening depending on the imposed spatial profile [4].

An initial investigation of the manufacturing variability introduced by the available 3D printed is presented. A total of 15 test samples were produced from Selective Laser Sintering (SLS). The test samples are 10 x 4 x 80 mm beam. The mass and dimensions of each sample were measured by a precision scale and a digital caliper, while the Young's modulus was measured by a universal test machine. The obatined mean value, standard deviation and coefficient of variation COV, i.e., the standard deviation over mean value, are presented in Table 1 for the mass density and Young's modulus. The samples dimensions shown negligible variability, which shows that the SLS is much more accurate for geometric than for material properties. Figure 3 presents the scatter plot of the mass density and Young's modulus of the 15 test samples. It can be clearly noticed that both material properties are correlated, most likely due to the porosity of the samples.

Table 1: The mean value, standard deviation and coefficient of variation COV of the density and Young's modulus of 15 test samples

	E, MPa	ρ, kg/m^3
Mean	1621.7	948.9
Standard deviation	49.9	7.4
COV, %	3.07	0.78

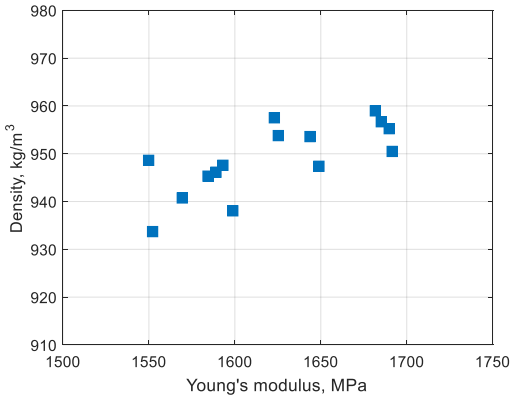

Figure 3: Scatter plot of the mass density and Young's modulus of the 15 test samples.

Note that the metastructure is 490 mm length with 17 unit cells. So the test samples are approximately 2.5 larger than the unity cell. It means that the material spatial variability of the test sample is avered out more significantly than for the unit cell

A metastructure of 490 mm total length is manufactured from the same SLS machine and it is assumed that it subject to the same manufacturing variability than the test samples. Note that, due to this design the test samples are approximately 2.5 larger than the unit cell, therefore the material spatial variability of the test sample is avered out more significantly than for the unit cell thus reducing the overall dispersion, as schematically shown in

3.1 Resonators mistuning

One of the most important effects for the vibration attenuation performance is the mistuning of the resonators [4], which is caused by the spatial profile on the material properties caused due to the manufacturing variability. In this section, the effects of the mistuning of resonators are numerically investigated. It assumed that all of the material variability can be represented by a change on the resonators mass, given by a lumped parameter in the analytical model.

To include the random spatial variability on the analytical model, a random field model is assumed based on available experimental results [4]. Random fields are multidimensional random processes and can be used to model spatially distributed variability using a probability measure [6]. The random field is Gaussian if its random variables are Gaussian and it is completely defined by its mean value, standard deviation and correlation function $C(\tau)$, where τ is the lag, i.e. the distance between any two points in the homogeneous random field.

It is assumed that the resonators mistuning can be represented by a variation on the tip masses of the resonators only. The manufacturing variability is assumed to be given by a Gaussian Homogeneous random field $H_1(x)$ and $H_2(x)$, for each mass, both with correlation function $C(\tau) = \exp(-\tau/c_l)$, where c_l is the correlation length, i.e., the level of statistical fluctuation of the spatial variability. In other words, this parameter controls the smoothness of the spatial variation, given the spatial profile of the tip masses of the resonators along the beam.

Due to the discrete nature of the resonators tip mass, the random fields $H_{1,2}(x)$ are discretized over the metamaterial length such that it is approximated by the random vector $\boldsymbol{\xi}$. The discretization process also results in a correlation matrix $\mathbf{C}$ from $C(\tau)$ [7]. This approach can also be used for the continuously varying material properties, like the Young's modulus, for instance. In this case, it is assumed that the material properties are constant within each unit cell. This approach is known as the midpoint method, first introduced by Der Kiureguian [8]. Let $\boldsymbol{\zeta}$ be a vector of uncorrelated Gaussian random zero mean and unit variance variables and with $\mathbf{C} = \langle \boldsymbol{\xi}\boldsymbol{\xi}^T \rangle$ the correlation matrix, where $\langle \cdot \rangle$ represents the mathematical expectation and T stands for transpose. This matrix is symmetric and positive-definite, so it is possible to apply a Cholesky decomposition of the kind $\mathbf{C} = \boldsymbol{\Sigma}\boldsymbol{\Sigma}^{\mathrm{T}}$, where $\boldsymbol{\Sigma}$ is a lower triangular matrix. A realization of the random field can be given by $\boldsymbol{\xi} = \boldsymbol{\Sigma}\,\boldsymbol{\zeta}$ [9], and the tip masses are given by a random vector

$$\mathbf{m}_{1,2} = \bar{\mathbf{m}}_{1,2}(\mathbf{1} + \sigma_H \boldsymbol{\xi}), \tag{3}$$

where $\bar{\mathbf{m}}_{1,2}$ is the nominal values of the resonators tip masses in the periodic design, $\mathbf{1}$ is a vector $m \times 1$ vector filled with 1 and σ_H controls the level of statistical dispersion of the random vector.

4. NUMERICAL RESULTS

In this section, a numerical analysis is carried out considering the mean value of density and Young's modulus given in Table **1**, Poisson ratio $\nu = 0.3$ and structural damping $\eta = 0.02$. Each cantilever beam or resonator, named 1 and 2, presented height $h_{s1} = 1.5$ mm, $h_{s2} = 2.5$ mm, width $b_{s1} = 2.0$ mm, $b_{s2} = 2.5$ mm and length $l_{s1} = l_{s2} = 21$ mm. The baseline beam presents a U-shaped cross-section with height $H_d = 10$ mm and width $w_d = 49$ mm, side wall thickness $t_d = 2$ mm, bottom plate thickness $b_d = 5$ mm and lateral plate thickness $t_w = 2$ mm distanced by $L_d = 15$ mm, with a total of 17 unit cell and total beam length $L = 257$ mm. The tip mass in both resonators at each unit cell is assumed to be 1 g. Note that, in this case, the different in length of the beams produces the differences in the resonance frequencies and therefore in the band gaps.

The effects of manufacturing uncertainty are considered on the tip mass of both resonators only, as described in section 3.1 assuming $c_l = 0.25L$ and $\sigma_H = 0.1$. First, the effects of individual samples of the metastructures are analysed and the physical consequences of the break in the periodicity is discussed.

Then the ensemble statistics are shown and discussed. Monte Carlo sampling is used as the stochastic solver with the number of samples necessary for adequate stochastic convergence.

Figure 4 presents the amplitude of the transfer receptance of proposed metastructure considering the nominal periodic design from 0 Hz to 350 Hz at steps of 0.5 Hz It can be seen that the two resonators design can effectively create two separate band gaps, significantly improving the vibration attenuation at more than one frequency band. It can also be noted that the produced stop band effect was created at very low frequency acting at the lowest modes of the structure. The attenuation performance of the band gaps can be given in terms of both the frequency band in which the attenuation occurs and in terms of the maximum attenuation at a specific frequency. Typically, a compromise between these both parameters can be sought for a optimum attenuation performance. Note that in the presented case, the total attenuation decreases 32 dB at both band gaps for a frequency width of $\Delta\omega_1 \approx 7$ Hz and $\Delta\omega_2 \approx 20$ Hz, for the lower and higher band gap, respectively. Moreover, both band gap presents similar performance considering $\Delta\omega_1/\omega_{01} \approx \Delta\omega_2/\omega_{02} \approx 9\%$.

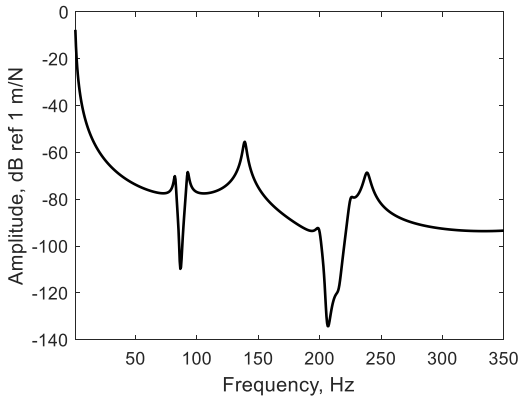

Figure 4: Amplitude of the transfer receptance of proposed metastructure considering the nominal periodic design.

Initially, it is considered that the tip masses of both resonators at each unit cell are identical, which is equivalent to assume that $\mathbf{m}_1 = \mathbf{m}_2$. Figure 5 presents the amplitude of the transfer receptance of the metastructure for some random samples from which two cases are highlighted in blue and red and have the corresponding tip masses spatial profile shown as well. Overall, it can be noticed that the mistuning resonators changed the vibration attenuation performance of the metastructure, as expected. The two highlighted cases present a qualitative difference in terms of band gap widening and maximum attenuation. The red case presents a smoother spatial profile when compared to the blue case, even though they present a very similar statistical dispersion and have been generated from the same random field family. The smoother spatial profile created band gaps with larger maximum attenuation in both band gaps, while the rougher spatial profile had a decreased maximum attenuation performance but a wider band gap. This difference is likely to have been generated by the wave trapping generated at the rougher profile [4]. The wave trapping is caused by a critical section [10], also known as a turning point [11], caused due to a transition from propagating to non-propagating waves along the beam at the same frequency. This transition causes a significant wave reflection even though the beam proprieties vary slowly [12].

Figure 6 also presents the amplitude of the transfer receptance of the metastructure for some random samples from which two cases are highlighted in blue and red, however, in this case, the tip masses at both resonators of each unit cell have independent realizations, i.e. $\mathbf{m}_1$ and $\mathbf{m}_2$ are independent random fields. A similar behaviour to the previous case can be observed in terms of the smoother and rougher spatial profile causing band gap widening and wave trapping, however in this case each band gap is affected in an independent manner. In the case highlighted in red, the tip mass spatial profile for the shorter cantilever beam is smoother than for the longer cantilever beam. Therefore, the corresponding

higher frequency band gap presents larger maximum vibration attenuation while the lower frequency band gap presents a lower maximum attenuation. For the case highlighted in blue, the opposite case happens, i.e. the tip mass related to the lower frequency band gap has a smoother spatial profile when compared to the other non-symmetric resonator. This effect causes the lower frequency band gap to present a better maximum attenuation performance that the second higher frequency band gap. These results shows that the both cantilever beams at each unit cell can be independently tuned for improved performance at each corresponding band gap.

Figure 7 presents the mean value and 5th and 95th percentiles of the amplitude of the transfer receptance of the metastructure for random samples considering $\mathbf{m}_1 = \mathbf{m}_2$ and independent realizations of $\mathbf{m}_1$ and $\mathbf{m}_2$. It can be noticed that for both cases, the uncertainty in the resonators affects mostly the band regions while slight affects the resonance peak between both stop bands. This response has been previously reported for other locally resonant metastructures (e.g. [13]) and shows that the structural modes are mostly unaffected by the uncertainty in the resonators. Moreover, the response statistics obtained from both cases are identical. This is because although individual samples are independent and can present significant performance changes, the statistical properties of both masses profiles are identical, i.e. both random vectors $\mathbf{m}_1$ and $\mathbf{m}_2$ have the same probabilistic measure.

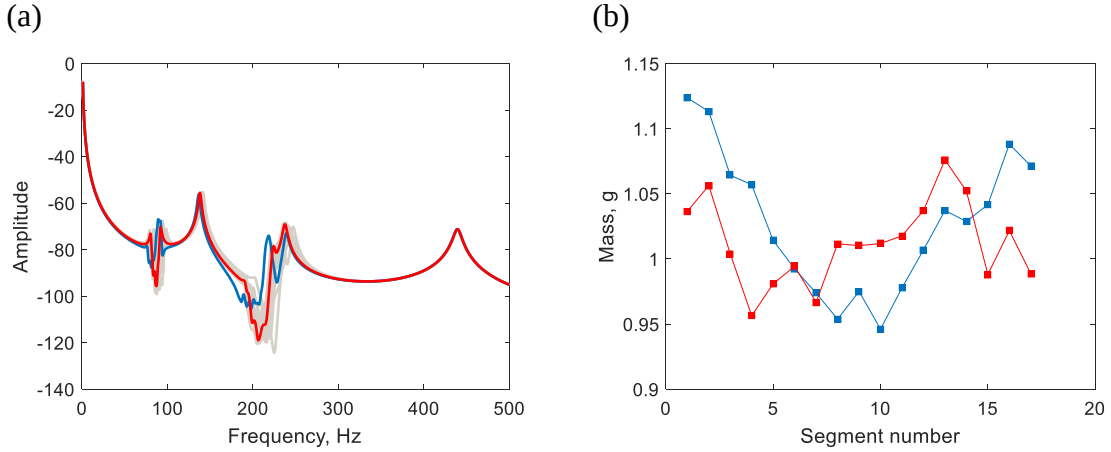

Figure 5: (a) Amplitude of the transfer receptance of the metastructure for random samples (grey) with highlighted cases (red and blue) and (b) the corresponding tip masses spatial profiles, considering $\mathbf{m_1} = \mathbf{m_2}$.

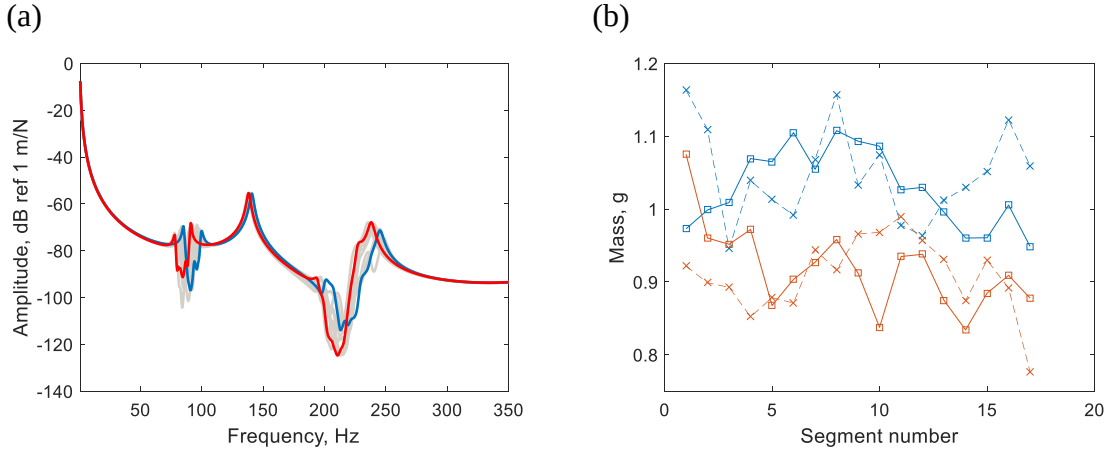

Figure 6: (a) Amplitude of the transfer receptance of the metastructure for random samples (grey) with highlighted cases (red and blue) and (b) the corresponding tip masses spatial profiles, considering independent realizations of $\mathbf{m_1}$ (dashed line with cross marker) and $\mathbf{m_2}$ (full line with square marker).

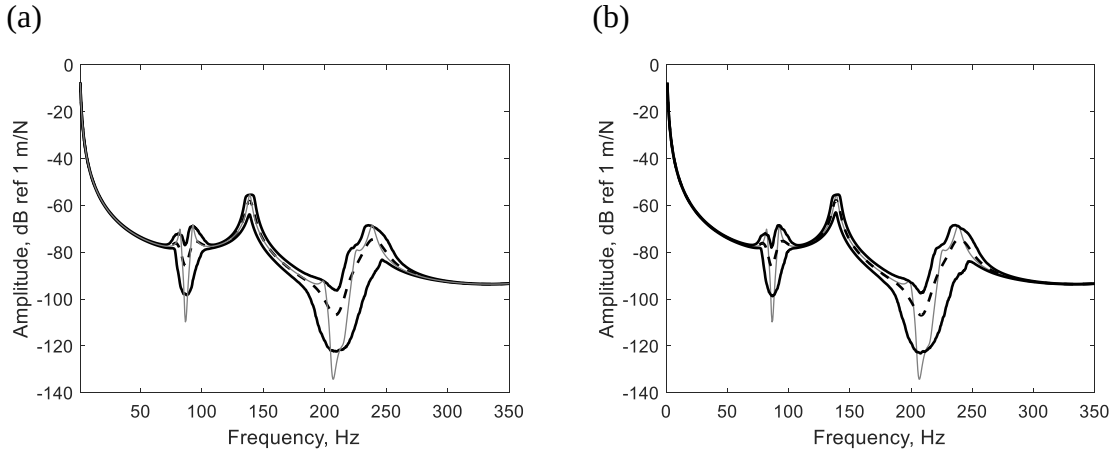

Figure 7: (a) The mean value and 5th and 95th percentiles of the amplitude of the transfer receptance of the meta-structure for random samples considering (a) $\mathbf{m_1} = \mathbf{m_2}$ and independent realizations of $\mathbf{m_1}$ and $\mathbf{m_2}$.

5. CONCLUDING REMARKS

In this work, manufacturing tolerances of beam samples produced from a Selective Laser Sintering process are assessed and variability levels are used to investigate the vibration suppression performance of broadband multi-frequency metastructures. An analytical model based on a transfer matrix approach is proposed to calculate transfer receptance due to a point time harmonic force of a metastructure designed with non-symmetric resonators in each unit cell. This configuration generated multifrequency attenuation due to each independent cantilever beam.

A random field model is proposed assuming all of the variability is due to the resonators cantilever beam tip mass. It is shown numerically that even for the same statistical properties, different spatial profiles can have a significant effect on the vibration attenuation performance in both band gaps, causing band gap widening, broadening the attenuation region, but decreasing the maximum attenuation when compared to the periodic response. These effects are related to wave trapping caused by critical sections, which can appear due to the resonators mistuning. Finally, the statistics of the response show that the band gap mistuning do not affect the structural modes. Most importantly, it is shown that the investigation of the uncertainty due to manufacturing has to take into account the spatial correlation of the properties of the metastructure resonators.

ACKNOWLEDGMENTS

The authors would like to acknowledge the support acquired by the H2020 DiaMoND project (Grant Agreement ID:785859), Royal Society Grant: PURSUIT, the Brazilian National Council of Research CNPq (Grant Agreement ID: 420304/2018-5) and the Federal District Research Foundation FAPDF (Grant Agreement ID: 0193.001507/2017).

REFERENCES

1. Bertoldi K, Vitelli V, Christensen J, van Hecke M (2017) Flexible mechanical metamaterials. Nature Reviews Materials 2:17066. https://doi.org/10.1038/natrevmats.2017.66
2. Fan Y, Collet M, Ichchou M, et al (2016) A wave-based design of semi-active piezoelectric composites for broadband vibration control. Smart Mater Struct 25:055032. https://doi.org/10.1088/0964-1726/25/5/055032
3. Sugino C, Xia Y, Leadenham S, et al (2017) A general theory for bandgap estimation in locally resonant metastructures. Journal of Sound and Vibration 406:104–123. https://doi.org/10.1016/j.jsv.2017.06.004
4. Beli D, Fabro AT, Ruzzene M, Arruda JRF (2019) Wave attenuation and trapping in 3D printed cantilever-in-mass metamaterials with spatially correlated variability. Scientific Reports Accepted for publication:
5. Fabro AT, Sampaio R, de Cursi ES (2019) Wave attenuation in a metamaterial beam assembly with uncertainties. In: Proceedings of the XVIII International Symposium on Dynamic Problems of Mechanics (DINAME2019). Buzios, Brazil

6. Vanmarcke E (2010) Random Field: Analysis and Synthesis, 2nd Revised and Expanded. Word Scientific, Cambridge, MA
7. Ghanem R, Spanos PD (2012) Stochastic Finite Elements: A Spectral Approach, Revised edition. Dover Publications, Minneola, N.Y.
8. Der Kiureghian A, Ke J-B (1988) The stochastic finite element method in structural reliability. Probabilist Engineering Mechanics 3:83–91
9. Rubinstein RY, Kroese DP (2007) Simulation and the Monte Carlo method, Second Edition. John Wiley & Sons, Inc., Hoboken, NJ, USA
10. Fabro AT, Ferguson NS, Mace BR (2019) Wave propagation in slowly varying waveguides using a finite element approach. Journal of Sound and Vibration 442:308–329. https://doi.org/10.1016/j.jsv.2018.11.004
11. John Heading (2013) An Introduction to Phase-Integral Methods, Reprinted edition. Dover Publications, New York, USA
12. Fabro AT, Ferguson NS, Jain T, et al (2015) Wave propagation in one-dimensional waveguides with slowly varying random spatially correlated variability. Journal of Sound and Vibration 343:20–48. https://doi.org/10.1016/j.jsv.2015.01.013
13. Beli D, Fabro AT, Ruzzene M, Arruda JRF (2016) Uncertainty analysis in vibroacoustic panels with band gap. In: ISMA 2016 Conference on Noise and Vibration Engineering. Leuven, Belgium, p 12